IUST International Journal of Engineering Science,
Vol. 19, No.5-1, 2008, Page 45-50

PREDICTION OF TEMPERATURE DISTRIBUTION IN THE HOT TORSION TEST SPECIMEN

B. Mirzakhani, M.T. Salehi, H. Arabi, S. Khoddam, S.H. Seyedein & M.R.Aboutalebi

Abstract: *Hot torsion test (HTT) has extensively been used to analysis and physically model flow behavior and microstructure evolution of materials and alloys during hot deformation processes. In this test, the specimen geometry has a great influence in obtaining reliable test results. In this paper, the interaction of thermal-mechanical conditions and geometry of the HTT specimen was studied. The commercial finite element package ANSYS was utilized for prediction of temperature distribution during reheating treatment and a thermo-rigid viscoplastic FE code, THORAX.FOR, was used to predict thermo-mechanical parameters during the test for API-X70 micro alloyed steel. Simulation results show that no proper geometry and dimension selection result in non uniform temperature within specimen and predicted to have effects on the consequence assessment of material behavior during hot deformation. Recommendations on finding proper specimen geometry for reducing temperature gradient along the gauge part of specimen will be given to create homogeneous temperature as much as possible in order to avoid uncertainty in consequent results of HTT.*

Keywords: *Temperature prediction, Hot torsion test, Simulation*

1. Introduction

The hot torsion test (HTT) has been one of the most popular mechanical tests for assessment of workability of metals and alloys for bulk forming processes during last decades [1-6]. The simple feature of the torsion test is that a constant true strain and true strain rate can be imposed by simply twisting one end relative to the other at a constant angular velocity. In this test, the specimens do not undergo significant shape change during deformation as long as the gage section is restrained to a fixed length. It is often chosen over the uniaxial tension and compression tests because very large strains and strain rates can be achieved without the problems of necking and barreling [7].

Paper first received Feb. 20, 2008, and in revised form Jau. 12. 2009.
B. Mirzakhani, Department of Metallurgical Engineering, IUST, Tehran, Iran, *bmirzakhani@iust.ac.ir*
M.T. Salehi, Department of Metallurgical Engineering, IUSTTehran, Iran. *salehi@iust.ac.ir*
H. Arabi, Department of Metallurgical Engineering, IUST, Tehran, Iran. *arabi@iust.ac.ir*
S. Khoddam, Mechanical Engineering Department, Monash University, Clayton Campus, Vic., Australia, *Shahin.Khoddam@eng.monash.edu.au*
S.H. Seyedein, Department of Metallurgical Engineering, IUST, Tehran. Iran, *seyedein@iust.ac.ir*
M.R. Aboutalebi, Department of Metallurgical Engineering, IUST, Tehran, Iran. *mrezab@iust.ac.ir*

However, to overcome the test rig limitations and to obtain the required strain and strain rate range, a wide range of specimen geometries and sizes have been used [1-6]. Failure to justify these choices may lead to some serious errors in deriving the constitutive parameters for a given material, due to the non-uniform temperature and localization of stress and deformation within gauge section of the test samples. These errors have not been investigated systematically.

The effect of pre-deformation reheating treatment on microstructure evolution such as initial austenite grain size and behavior of microalloying elements has been investigated in several studies [6, 8-12].

These investigations deduce that austenitizing temperature has a great influence on initial microstructure and consequence deformation behavior of steels. In hot torsion machines the heating energy usually is supplied by an induction or resistance type furnace [1-3, 13-15]. The influences of specimen geometry of HTT and heating conditions have not been investigated systematically. However, no proper consideration of these choices may introduce some errors in consequence results of test due to the non-uniform temperature and microstructure within the material.

In the present study, the commercial finite element package ANSYS was used to predict temperature distribution within the specimen during reheating treatment. A thermo-rigid viscoplastic FE code,

THORAX.FOR, was also developed to calculate thermal-mechanical parameters during the test.

2. Model and Simulation Conditions

According to reheating treatments which almost is used in experiments, a reheating cycle was designed as shown in Fig.1. The temperatures 740 and 880 ºC in this figure are Ac1 and Ac3 temperatures of present microalloyed steel respectively which were determined by dilatometry test. In this range rather low heating rate considered in order to give time for ferrite and perlite transformation to austenite. The commercial FEM code ANSYS was used to predict temperature distribution during reheating treatment and a thermo-rigid viscoplastic FE code, THORAX.FOR, was utilized to calculate thermal-mechanical parameters during the HTT.

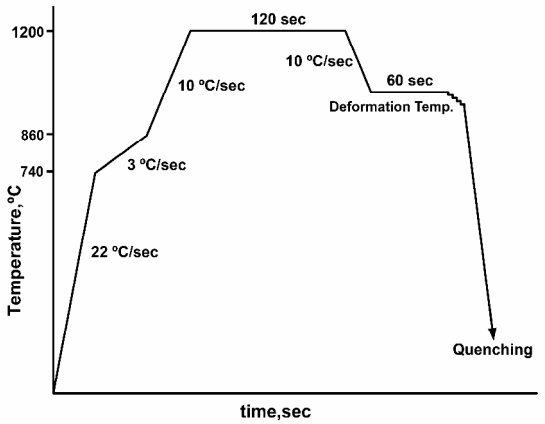

Fig. 1. The reheating cycle before hot torsion test

A two dimensional FE analysis of heat flow was used here to study the interaction of specimen geometry and thermal-mechanical conditions. The domain, boundaries and the mesh which were used is also presented in Fig. 2a where only half of a longitudinal section of Fig. 2b is considered because of the symmetry of geometry and the condition with respect to r and z axis.

The axisymmetric conditions between the body and its environment imply that heat flux along the boundaries S1 is zero or insulated.

The boundary S2 is directly heated by an induction coil of 45 mm length. The heating was controlled by a pyrometer carefully located above the center of the specimen. The boundary S3 is exposed to the surrounding environment where the energy loss is considered through both boundary convection and radiation.

The boundary S4 is in contact with grippers of the HTT machine. For these boundaries, the thermal contact conductance of the interface between the specimen and the grips was considered and heat exchange modeled by convection.

Different HTT specimens were considered. In the first set of samples, the gauge lengths were 8, 33, 42 and 52 mm and the gauge radius was 3.35mm named G1, G2 and G3 respectively. For the second set of the samples, the radii were 2.5, 3.35 and 4.25mm and the length was 42mm named G5, G3 and G6 respectively. It should be noted that the relationship between the sizes of the specimen, as shown in Fig. 2b, were designed according to the basic stiffness requirement expressed in [16, 17].

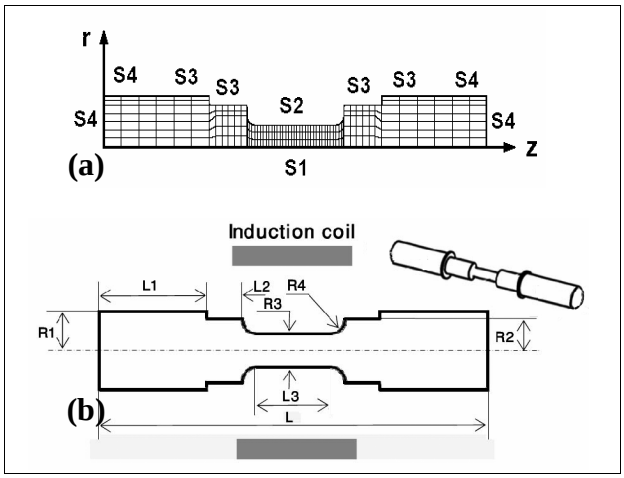

Fig. 2. a) The domain, boundaries and mesh of modeling and b) Schematic of geometry of a solid hot torsion specimen

For solution of thermal problem during deformation the energy balance equation was used:

$$\frac{\partial q_x}{\partial x}+\frac{\partial q_y}{\partial y}+\frac{\partial q_z}{\partial z}-Q+\rho c\frac{\partial T}{\partial t}=0 \qquad (1)$$

where q_x, q_y and q_z are components of the heat flow rate vector per unit area in Cartesian coordinates (x, y, z), *t*, *T* and *Q* are time, temperature and the heat generated due to plastic work respectively. The amount of *Q* can be estimated as:

$$Q=\kappa\sigma_{ij}\varepsilon_{ij} \qquad (2)$$

where κ is the heat generation efficiency that is assumed to be 0.9 in this work [18]. In fact, this term has an important role in raising temperature of the sample during deformation process especially at high deformation rates.

A simplified approach for radiation heat transfer was utilized by using an equivalent convection boundary condition in which the non-linearity is considered through a temperature-dependent convection coefficient which will be designated here as h_r:

$$h_r=\breve{\sigma}\varepsilon\left[\left(T_s^2+T_{se}^2\right)\left(T_s+T_{se}\right)\right]_{n-1} \qquad (3)$$

where h_r is equivalent convection coefficient between the body surface S and the surface of the environment enclosing the body at the n^{th} time step, T_s and T_{se} are the absolute temperatures in degrees Kelvin between these surfaces, $\breve{\sigma}$ is Steffan-Boltzman coefficient and ε emissivity factor of the surface. The value of $\varepsilon = 0.65$ was determined according to the ASTM standard test [19].

3. Results and Discussion

The temperature history of two points on the surface in the center and end of gauge section of G3 during reheating treatment is presented in Fig. 3. It shows that the desirable reheating cycle was only obtained at the center of specimen.

The ends of gauge section not only did not reach to appropriate temperature for starting deformation but also the desired reheating temperature, i.e. 1200ºC, at the ends did not achieve. So, it is expected that the solution of the chemical elements will not be occurred completely at these areas. This would fail achievement of a homogeneous composition within specimen before deformation. In addition, different austenitizing temperature at different points of the specimen leads to various initial grain sizes of austenite which is a critical factor that influences subsequent deformation behavior and phase transformation of steel [8-12].

Fig. 4 shows the contour plots of temperature distribution in various geometries of HTT specimens after applying reheating cycle (Fig.1) and before starting deformation at 1000ºC. This figure illustrates that inductive heating may produce non uniform temperature along the axis of the specimens and caused temperature gradient within gauge part of the sample. In that, in specimens having longer gauge, show greater thermal gradient.

For example in G4 (52mm gauge length) the temperature differential between center and end of the gauge is the largest and about 160ºC. It should be noted that for all specimens the induction length assumed to be constant and was equal to 45mm. Sections of specimens located outside of induction coil absorbed the heat of the inside sections and led to lower temperature of ends than center of gauge.

This result indicates assumption of uniform temperature distribution in the gauge part of the specimen mentioned in previous works [13, 14, 16, 18] may not be valid. This would have a negative impact on the final results of the test.

For evaluation of the effect of gauge length on maximum differential temperature along the gauge section and obtain optimum sample geometries, the value of temperature difference between the gauge center and gauge was calculated for various specimens at different temperatures and plotted in Fig. 5. This figure indicates as the gauge length increased; the temperature gradient increased; so that for specimen with 52mm gauge length this gradient exceeded 200ºC at 1100ºC.

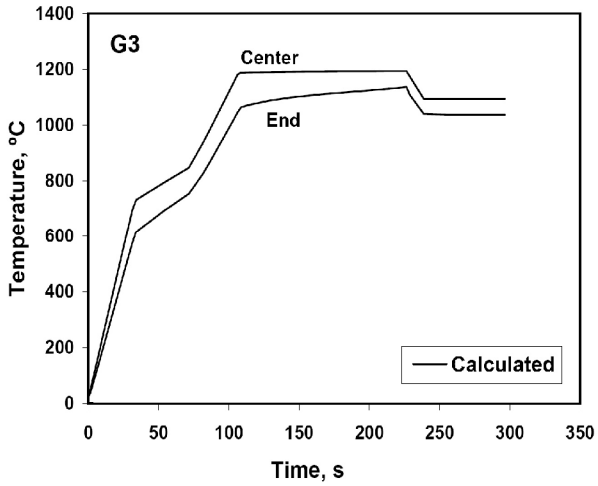

Fig. 3. The time history of two points in the gauge section of G3 during reheating treatment

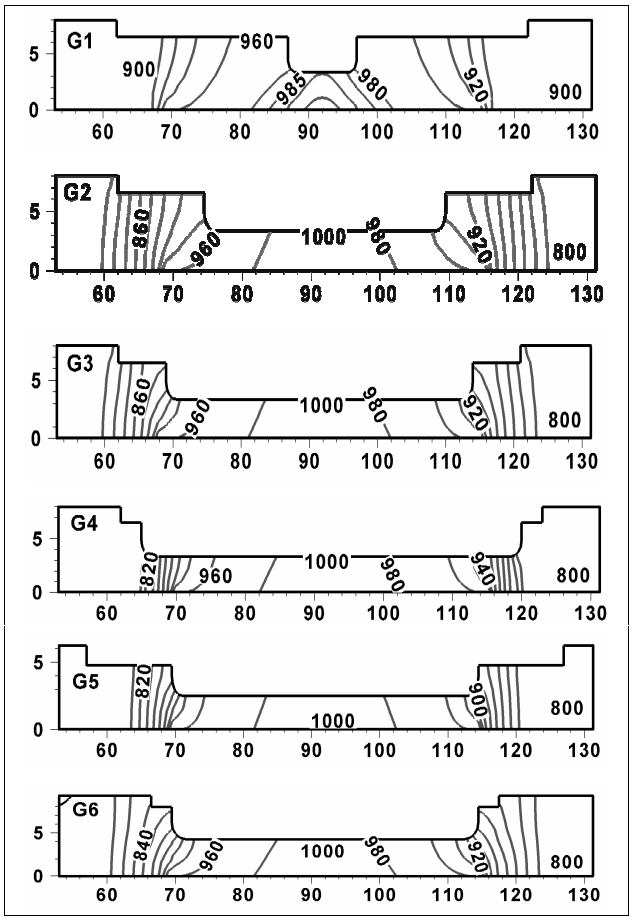

Fig. 4. Initial temperature distribution in G1, G2, G3, G4, G5, G6, after applying reheating cycle.

It can be also observed that the temperature gradients prior to start of deformation at different temperature are not similar. On the other hand, as temperature of final step decreased the gradient decreased. It relates to the temperature difference between gauge section and

other part of the specimen which is less at lower temperatures than higher temperatures. For specimen with short gauge length the temperature did not show much influence on temperature gradient along the sample. Fig. 6 shows the temperature difference between the surface and the core of the sample at the center and the end of gauge section after reheating and before the start of deformation at 900ºC, 1000ºC and 1100ºC. As illustrated in this figure, there is a temperature gradient along the specimen radius because of heat transfer via convection and radiation from surface to the surrounding medium. But radial variation of temperature was much less at the center than at the ends of gauge section. It is due to the ends of gauge section that are not only adjacent to the end of induction coil but also they are connected to the mini-shoulders and shoulders which absorb a considerable amount of heat generated in the gauge section.

As shown in Fig. 6, when reheating treatment finished at 1100ºC the maximum redial gradient at both center and ends of gauge was greater in comparison to of 1000ºC and 900ºC. However at the center of specimen, temperature difference between surface and core of gauge were less than 45ºC and 15ºC respectively at 1100ºC. For a given reheating cycle, geometry of HTT specimen has a great influence on temperature distribution after reheating treatment and before deformation as shown in Fig. 4-6. Various geometries experienced different temperature distribution.

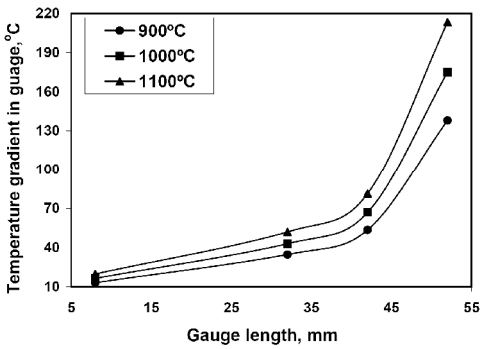

Fig. 5. Effect of gauge length on maximum differential temperature along the gauge section

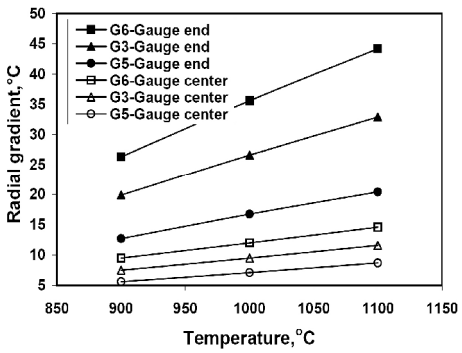

Fig. 6. Temperature difference between the surface and the core of the sample at the center and the end of gauge before the start of deformation at 900ºC, 1000ºC and 1100ºC

Fig. 7 displays the contour plot of temperature distribution with different specimen geometries deformed at 1000ºC with a twist rate of ω=3 rad.sec^{-1}. Comparing Fig.4 and Fig. 7, one could see how temperature distribution has changed after deformation. In all specimens except G5 temperature increased at the center of gauge section because of heat generation due to the plastic deformation work. However in specimens with 42mm and 52mm gauge length, temperature decreased at the other points of gauge section. It can be seen from the results that by increasing the gauge length, the thermal gradient along specimen axis increases after deformation. It could be explained by the long deformation time required for long specimens to reach required strain. During this time, a considerable heat will be lost by different modes of heat transfer through the mini-shoulders, shoulders and the environment.

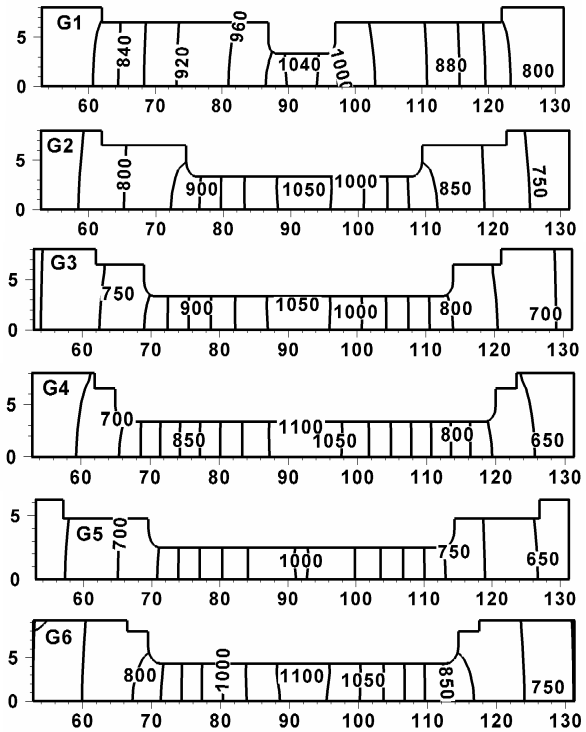

Fig. 7. Temperature distribution in G1, G2, G3, G4, G5, and G6 deformed at 1000ºC and ω=3 rad.sec-1

The finite element calculations shown in Fig. 7, indicate that for the cases investigated, temperature variations in the radial direction were negligible (about 10ºC) within the gauge part of all specimens. However, the strain and strain rate variations between the center and surface of specimen are significant. Fig. 8 shows the variations of strain contours for G4 deformed at 1100ºC, ω= 10 rad.sec-1 and the effective strain of 3.0. It should be noted that in torsion test there is the radial variation of the strain and strain rate. It makes interpretation of torsion-test data more complex. Meanwhile the given effective strain is applied in the surface of the specimen.

These may be explained by noting that for high twisting rates, the deformation time is very short and a high amount of heat is produced in the gauge section at the center of the specimen.
During deformation, this heat can not be transferred fast enough to the interfacing shoulders and the environment. In addition the ends of the gauge section in the long specimen, G4, are at lower temperature compared to the center of the gauge section. Consequently, due to a high temperature gradient in longitudinal direction and a considerable strain/strain rate change in the gauge section, flow localization will happen (Fig. 9).
This involves the mid-gauge section experiencing softening phenomenon, i.e. dynamic recrystallization, during deformation because of high temperature and strain of this region; while the ends of the gauge section can not flow as easily as the center. This results in flow localization. It could be concluded that long specimens deformed at high twisting rates are more susceptible to flow localization. In such cases, flow localization is unavoidable, and the obtained flow curve of the material includes significant post processing error. Careful selection of the specimen geometry and twist rate leads to a minimum temperature gradient in the gauge section before and during the deformation and therefore, will minimize this problem.
This might not be always achievable as for representing an industrial forming process with a given strain rate, a given combination of the specimen geometry and twist rate is needed which do not necessarily match those of the optimized geometry and twist rate from the flow localization point of view. In order to reduce temperature variations in the gauge section of a long specimen, and consequently to minimize flow localization in the hot torsion test involving high strain rates, one may apply a non-uniform heat in the longitudinal direction. This however could have a negative impact on distribution of chemical composition within the materials.

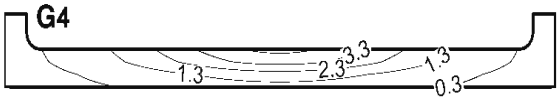

Fig. 8. Effective strain contour plot in G4 deformed at 1100ºC and ω= 10 rad.sec-1

Fig. 9. Flow localization in the G4 specimen deformed at 1100ºC and ω= 10 rad.sec-1 after applying the reheating cycle

In this study, results show that no proper geometry and dimension selection result in non uniform temperature within specimen. It may affect the consequence assessment of material behavior during hot deformation as seen in Fig. 9. In addition, it seems prevention of any temperature gradient during reheating treatment of HTT is un-avoidable, but choosing an optimum geometry will minimize this problem. Among different geometries, the specimens G1 and G2 showed the low temperature gradient in both axis and radial directions of the gauge section. Therefore it can be concluded that the optimum specimens' length are between 0.2 and 0.7 of induction coil.

4. Conclusion

A numerical modelling was performed to analysis interaction of geometry of hot torsion test specimens and thermal conditions for API-X70 microalloyed steel by the commercial finite element package ANSYS and a thermo-rigid viscoplastic FE code. Results showed that the specimens having between 0.2 and 0.7 length of induction coil experienced low temperature gradient in both axial and radial directions after reheating treatment. It seems these geometries are more reliable for driving accurate constitutive parameters of the steel by hot torsion test.

Acknowledgment

The first author is grateful for the Arak University provided scholarship. In addition, the authors would like to acknowledge the contributions of Mr. A. Abdolhosseini and Mr. Y.A. Mohammadi.

References

[1] Samuel, F.H., Yue, S., Jonas, J.J., Zbinden, B.A., "*Modeling Testing of Flow Stress and Rolling Load of a Hot Strip Mill by Torsion*." ISIJ International, Vol. 29, 1989, pp. 878-886.

[2] Bia, D.Q., Yue, S., Sun, W.P., Jonas, J.J., "*Effect of Deformation Parameters on the No-Recrystallization Temperature in Nb-bearing Steels*", Metallurgical Transactions A, Vol. 24A, 1993, pp. 2151-2159.

[3] Carsi, M., Lopez, V., Penalba, F., Ruano, O.A., "*The Strain Rate as a Factor Influencing the Hot Forming Simulation of Medium Carbon Microalloyed Steels*", Materials Science and Engineering A, Vol. A216, 1996, pp. 155-160.

[4] Hodgson, P.D., Kong, L.X., Davies, C.H.J., "*The Prediction of the Hot Strength in Steels With an Integrated Phenomenological and Artificial Neural Network Model*", Journal of Materials Processing Technology, Vol. 87, 1999, pp. 131-138.

[5] Quispe, S.F., "*Improved model for Static Recrystallization Kinetics of Hot Deformed Austenite in Low Alloy and Nb/V Microalloyed Steels*", ISIJ International, Vol. 41, 2001, pp. 174-781.

[6] Kuc, D., Niewielski, G., Cwajna, J., "*Influence of Deformation Parameters and Initial Grain Size on the Microstructure of Austenitic Steels After Hot-Working*

Processes", Materials Characterization, Vol. 56, 2006, pp. 318-24.

[7] Dieter, G., Howard, A., Kuhn, S., Semiatin, L., Handbook of workability and process design, ASM, 2003.

[8] Tanaka, T., Enami, T., Kimara, M., Saito, Y., Hatomura, T., *"Formation Mechanism of Mixed Austenite Grain structure Accompanying Controlled- Rolling of Niobium-Bearing Steel*", Proceeding of International Thermomechanical of Microalloyed Austenite, 1981, pp. 195-215.

[9] Yoshie, A., Fujioka, M., Watanabe, Y., Nishioka, K, Hirofumi, M., *"Modelling of Micro Structural of steel Plates Produced by Evolution and Mechanical Properties Thermo-Mechanical Control Process*", ISIJ International ,Vol. 32 No, 3, 1992, pp. 395-404.

[10] Flores O., Martinez, L., "*Abnormal Grain Growth of Austenite in a V-Nb Microalloyed Steel",* Materials Science, Vol. 32, 1997, pp. 5985- 5991.

[11] Fernandez, A.I., Lopez, B., Rodriguez-Ibabe, J.M., *"Static Recrystallization Mechanisms in a Coarse-Grained Nb-Microalloyed Austenite*", Metallurgical and Materials Transactions A, Vol. 33A, 2002, pp. 3089-3098.

[12] Oudin, A., Barnett, M.R., Hodgson, P.D., *"Grain Size Effect on the Warm Deformation Behavior of a Ti-IF Steel",* Materials Science and Engineering A, Vol. 367, 2004, pp. 282-294.

[13] Zhou, M., Clode M.P., *"A Finite Element Analysis for the Least Temperature Rise in a Hot Torsion Test Specimen*", Finite Elements in Analysis and Design, Vol. 31, 1998, pp. 1-14.

[14] Njiwa, R.K., Metauer, G., Marchal, A., Stebut J.V., "*Effect of Self Heating on the Torque vs. Equivalent Tensile Strain Plot in High Temperature Torsion of Visco-Plastic Material",* Journal of Materials Science, Vol. 36, 2001, pp. 5659-5663.

[15] Khoddam, S., Hodgson P.D., *"Conversion of the hot Torsion Test Results into Flow Curve with Multiple Regimes of Hardening"*, Journal of Materials Processing Technology, Vol. 153-154, 2004, pp. 839-845.

[16] Khoddam, S., Lam, Y.C., Thomson, P.F., "*The Effect of Specimen Geometry on the Accuracy of the Constitutive Equation Derived rom the Hot Torsion Test*." steel research, Vol. 66, No. 2, 1995, pp. 45-49.

[17] Shigley, J.E., Mitchell, L.D., *Mechanical Engineering Design*, McGraw-Hill, New York, 1983.

[18] Kobayashi, S., Oh, S. I., Altan, T., *.Metal Forming and the Finite Element Method* ,Oxford University Press, 1989.

[19] User guide of OS550/OS550-BB series industrial infrared thermometer/transmitter, Appendix C: Determining an unknown emissivity, Omega, the USA, 2001, p. c-1.